



HAL
open science

Analysis of liver viscosity behavior as a function of multifrequency magnetic resonance elastography (MMRE) postprocessing

Gwladys E Leclerc, Ludovic Robert, Marie-Christine Ho Ba Tho, Colette Rhein, Jean-Paul Latrive, Sabine F Bensamoun, Fabrice Charleux

► **To cite this version:**

Gwladys E Leclerc, Ludovic Robert, Marie-Christine Ho Ba Tho, Colette Rhein, Jean-Paul Latrive, et al.. Analysis of liver viscosity behavior as a function of multifrequency magnetic resonance elastography (MMRE) postprocessing. *Journal of Magnetic Resonance Imaging*, 2013, 38, pp.422 - 428. 10.1002/jmri.23986 . hal-03809995

HAL Id: hal-03809995

<https://utc.hal.science/hal-03809995v1>

Submitted on 11 Oct 2022

HAL is a multi-disciplinary open access archive for the deposit and dissemination of scientific research documents, whether they are published or not. The documents may come from teaching and research institutions in France or abroad, or from public or private research centers.

L'archive ouverte pluridisciplinaire **HAL**, est destinée au dépôt et à la diffusion de documents scientifiques de niveau recherche, publiés ou non, émanant des établissements d'enseignement et de recherche français ou étrangers, des laboratoires publics ou privés.

Original Research

Analysis of Liver Viscosity Behavior as a Function of Multifrequency Magnetic Resonance Elastography (MMRE) Postprocessing

Gwladys E. Leclerc, PhD,¹ Fabrice Charleux, MD,² Ludovic Robert, MS,² Marie-Christine Ho Ba Tho, PhD,¹ Colette Rhein, MD,³ Jean-Paul Latrive, MD,⁴ and Sabine F. Bensamoun, PhD^{1*}

Purpose: To analyze the relevance of the viscosity measurement as a liver diagnostic marker.

Materials and Methods: To determine the level of fibrosis, a Fibroscan test was performed on 40 subjects (10 healthy volunteers and 30 patients). Subsequently, multifrequency magnetic resonance elastography (MMRE) tests were made with a pneumatic driver at 60, 70, and 80 Hz. Phase images were analyzed with two different postprocessing methods, without (Method 1) and with (Method 2) the inversion algorithm (IA), using rheological models (Voigt, springpot) in order to characterize the viscoelastic properties (viscosity: η and elasticity: μ).

Results: MRE cartography of the viscous tendency (G'_{MRE_M2}) measured within the region of interest (ROI) of the liver increased as a function of the level of fibrosis. Similar results were also obtained for the viscosity (η_{models_M1}) calculated with a postprocessing without IA. However, the viscosity (η_{models_M2}) remained constant with the stage of fibrosis when the postprocessing was composed of an IA. The experimental (μ_{MRE_M1} and G'_{MRE_M2}) and rheological (μ_{models_M2} and μ_{models_M1}) elasticities always increased with the level of fibrosis regardless of the postprocessing method.

Conclusion: The variation of the liver viscosity parameter as a function of postprocessing revealed that this parameter should be further investigated to demonstrate its relevance in clinical practice.

Key Words: multifrequency magnetic resonance elastography; liver fibrosis; viscosity; elasticity; rheological models

J. Magn. Reson. Imaging 2013;38:422–428.

© 2013 Wiley Periodicals, Inc.

SOME LIVER DISEASES are still underdiagnosed with blood tests due to the lack of specific markers, and are also underestimated with biopsy, which revealed a sample error of 25% (1). The development of noninvasive imaging tools has improved the diagnosis of liver fibrosis allowing for long-term follow-up of patients. Indeed, the ultrasound elastography and magnetic resonance elastography (MRE) methods, based on wave propagation, characterized the liver tissue through the measurement of two main parameters, elasticity and viscosity, representing the global elasticity of the liver and the microstructural changes, respectively.

Liver stiffness (elasticity) was widely characterized for healthy (2–4) and pathological (5,6) livers through measurement of the Young's modulus (E) parameter using ultrasound elastography (Fibroscan, supersonic shear imaging) and through measurement of the shear stiffness ($\mu = E/3$) parameter using the MRE technique. Ultrasound elastography provided a local liver stiffness compared to MRE, which revealed a cartography of the liver shear stiffness (μ) enabling the radiologist to analyze the spatial elasticity distribution and to select different regions of interest (ROIs) (6–8). All of the previous elastography studies have demonstrated an increase of the liver stiffness as a function of liver fibrosis (9) and specific cutoffs were established (5,10).

To further characterize the microstructural changes, the viscosity (η) parameter was analyzed with MRE associated with different methods using inversion algorithms (11) and rheological models (12–14). The advantage of using an inversion algorithm, involved in magnetic resonance imaging (MRI) postprocessing, was to provide a spatial representation of the trend of liver viscosity (12–14). Subsequently, the closest viscosity exhibited by the liver in real life was obtained with multifrequency MRE (MMRE) tests associated with different solid (Voigt, Zener, springpot) or fluid (Maxwell and Jeffreys) rheological models (12,15). In the literature, healthy (15) and pathological (12,16) livers revealed different ranges of viscosity as a function of postprocessing (eg, inversion algorithm, rheological model).

¹Université de Technologie de Compiègne, UMR CNRS 7338, BioMécanique et BioIngénierie, Compiègne, France.

²Radiology Unit, ACRIM-Polyclinique Saint Côme, Compiègne, France.

³CH Compiègne, Unité d'alcoologie, Compiègne, France.

⁴CH Compiègne, Service Gastro-entérologie et Hépatologie, Compiègne, France.

*Address reprint requests to: S.F.B., Université de Technologie de Compiègne (UTC), Centre de recherches de Royallieu, Laboratoire de BioMécanique et BioIngénierie, UMR CNRS 7338, Rue Personne de Roberval, BP 20529, Compiègne Cedex, France.
E-mail: sabine.bensamoun@utc.fr

Received August 1, 2012; Accepted November 8, 2012.

DOI 10.1002/jmri.23986

View this article online at wileyonlinelibrary.com.

At the present time the liver stiffness measurement is clinically used to diagnose the level of liver fibrosis, and in the near future the viscosity will also be of use as a diagnostic marker. Thus, the purpose of this study was to raise the relevance of the viscosity compared to the clinical elasticity and to analyze the effects of the postprocessing (inversion algorithm, rheological models) on this parameter.

MATERIALS AND METHODS

Subjects

Forty subjects comprised of 10 healthy volunteers (seven men, three women, mean age, 41 years; range, 23.8–48.4 years) without liver damage, and 30 alcoholic patients (23 men, 7 women, mean age, 43 years; range, 29.6–59.8 years) were recruited from the alcoholism department. Each subject underwent two elastography (Fibroscan, MRE) exams in a row. Exclusion criteria were claustrophobia, mental instability, existence of hepatitis, suspicion of hemochromatosis, and invalidated Fibroscan test. This prospective study was approved by the Institutional Review Board and written informed consent was obtained.

Ultrasound Elastography

Biopsy being a risky and unnecessary procedure for alcoholic patients, the Fibroscan (EchoSens, Paris, France) exam was used as the reference technique to identify the level of fibrosis (F) (10) and the distribution was F1 ($n = 10$), F2 ($n = 10$), F3 ($n = 5$), F4 ($n = 5$). During the Fibroscan test, an ultrasound probe composed of a vibrator was placed between intercostal spaces and low-frequency (50 Hz) waves were generated. The liver elasticity (Young's modulus: $E_{\text{Fibroscan}} = 3 \cdot \mu_{\text{Fibroscan}}$, μ : shear stiffness) was locally measured with 20 validated measurements (3).

MMRE

The subjects lay supine in a 1.5T MRI machine (GE, Milwaukee, WI) and a clinical acoustic driver, connected to a large active loudspeaker, was placed at the same level as the diaphragm and positioned in contact with the ribcage. Subsequently, MMRE experiments were performed at 60, 70, and 80 Hz and shear waves were propagated within the liver. The applied range of frequencies was chosen according to Leclerc et al's analysis (17), who had characterized the material properties of the present driver.

Phase images (Fig. 1A,B) revealing the wave displacement within the liver were recorded with two offsets in a row, a motion sensitizing gradient echo sequence, a flip angle of 30°, a field of view between 36 and 48 cm, a 256 × 64 acquisition matrix, a TE corresponding to the minimum echo time allowing for motion encoding, and a TR equal to 100 msec. For each frequency the total scan time was 32 seconds, corresponding to two breath-holding periods of 16 seconds.

MMRE Postprocessing

Methods

In order to analyze the impact of the MMRE postprocessing on the viscoelastic (elasticity: μ and viscosity: η) properties of the liver, the phase images were analyzed with two different methods.

Method 1, which did not use an inversion algorithm (IA), provided a local analysis of the liver elasticity. Indeed, a profile was prescribed (Fig. 1A) in the direction of the shear wave propagation allowing the local measurement of the shear wave velocity ($V = f \cdot \lambda$) along the profile from the wavelength (λ) and the applied frequency (f). Moreover, assuming that the liver tissue was linear elastic, isotropic, and homogeneous, the local shear stiffness (μ_{M1}) representing the local elasticity of the liver was also calculated (Fig. 1A) for each frequency using the following equation $\mu_{MRE_M1} = \rho \cdot V^2 = \rho \cdot (f \cdot \lambda)^2$, where ρ is the liver density (1000 kg/m³).

Method 2 applied an inversion algorithm to the phase images providing two cartographies termed G' and G'' , representing the global tendency of the elasticity and the viscosity of the liver, respectively (Fig. 1B). The purpose of the inversion algorithm was to inverse the Helmholtz equation in order to obtain the viscoelastic properties from the displacement of the shear waves (11). Then ROIs were prescribed on both cartographies allowing an average assessment of the trend of the viscoelastic (G'_{MRE_M2} , G''_{MRE_M2}) properties. It must be noted that a shear complex modulus (labeled: G^*) was obtained by the sum of G' and G'' corresponding to the real and the imaginary components (Fig. 1B).

Cost Functions

Subsequently, the quantification of the shear stiffness (μ) and the viscosity (η) were performed with the minimization of two cost functions J_{M1} (Eq. 1) and J_{M2} (Eq. 2), based on a mean squared analysis (17), related to Method 1 and Method 2, respectively (Fig. 1C,D).

J_{M1} was defined with the Helmholtz equation as the difference between the experimental and rheological velocities (V_{G^*}) (Fig. 1C) (18):

$$J_{M1} = \frac{1}{2}(V_{G'} - V_{60\text{Hz}})^2 + \frac{1}{2}(V_{G'} - V_{70\text{Hz}})^2 + \frac{1}{2}(V_{G'} - V_{80\text{Hz}})^2 \quad \text{with} \quad V_{G^*}^2 = \frac{2 \cdot |G^*|^2}{\rho \cdot (|G^*| + \text{Re}(G^*))} \quad [1]$$

J_{M2} was composed of the difference between the imaginary (Im) and real (Re) parts of the shear complex modulus (G^*) (Fig. 1D):

$$J_{M2} = [\text{Re}(G^*) - \text{Re}(G_{60\text{Hz}}^*)]^2 + [\text{Im}(G^*) - \text{Im}(G_{60\text{Hz}}^*)]^2 + [\text{Re}(G^*) - \text{Re}(G_{70\text{Hz}}^*)]^2 + [\text{Im}(G^*) - \text{Im}(G_{70\text{Hz}}^*)]^2 + [\text{Re}(G^*) - \text{Re}(G_{80\text{Hz}}^*)]^2 + [\text{Im}(G^*) - \text{Im}(G_{80\text{Hz}}^*)]^2 \quad [2]$$

Rheological Models

Two different solid rheological models (Voigt and springpot, Fig. 1E) were used to define the shear complex modulus (G^*_{Voigt} or $G^*_{\text{springpot}}$) in both cost

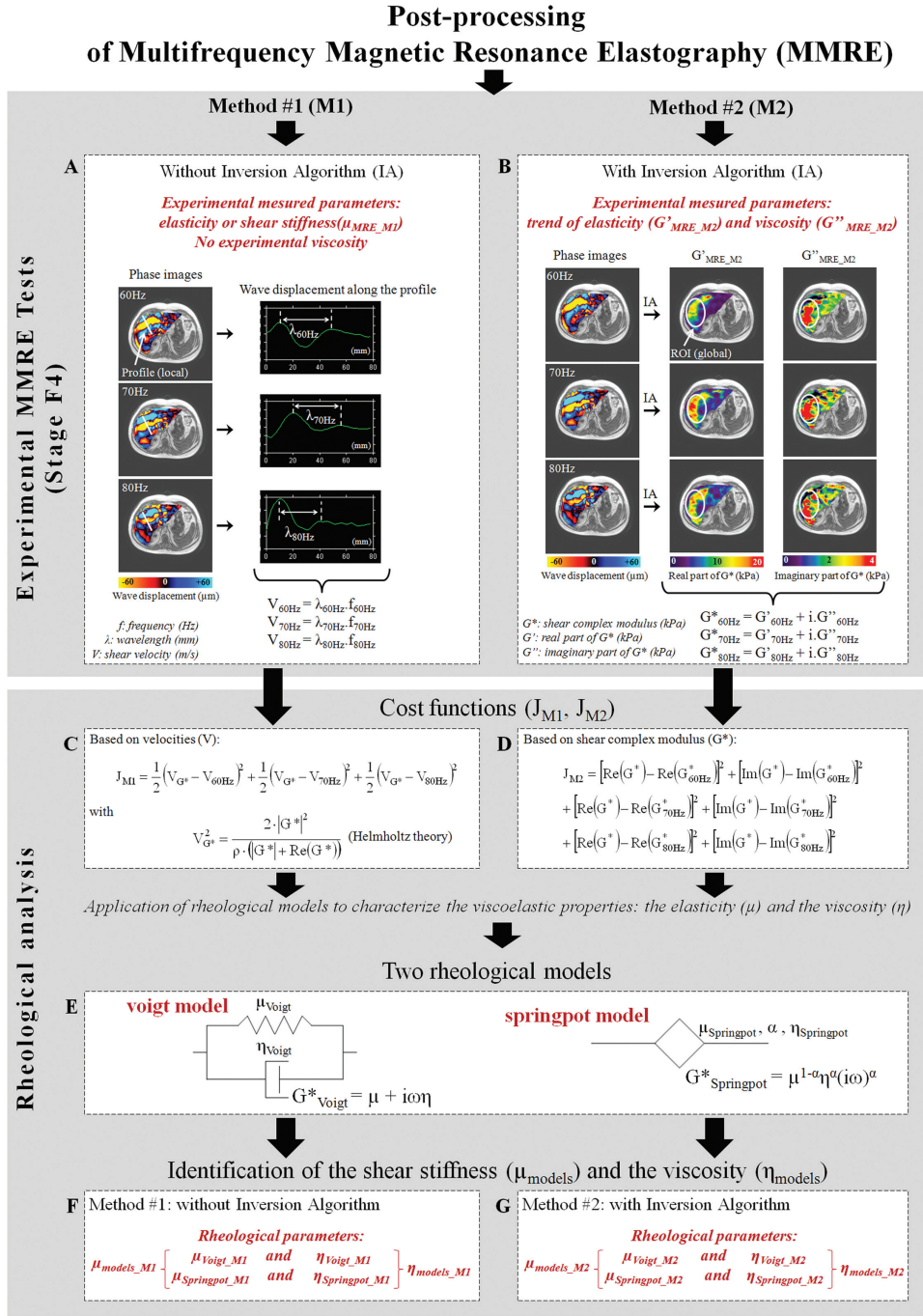


Figure 1. Diagram of the different steps represented MMRE postprocessing. The experimental part was composed of MMRE tests where the phase images were analyzed with two different methods, M1 and M2, made without (A) and with (B) inversion algorithm, respectively. The rheological analysis was composed of three main phases composed of two cost functions, J_{M1} and J_{M2} (C,D), two rheological models (Voigt and springpot) (E) and an identification process (F,G) allowing for the measurement of the viscoelastic (μ : elasticity, η : viscosity, and α for springpot model) properties of the liver.

functions related to the shear stiffness (μ_{Voigt} , $\mu_{\text{Springpot}}$) and to the viscosity (η_{Voigt} , $\eta_{\text{Springpot}}$) (Fig. 1F,G).

The Voigt model was chosen as a referent rheological model for its simple composition (one dashpot and one spring) and also for its common use to characterize the viscoelastic properties of biological tissues. In addition, a more complex model (springpot), composed of a third parameter (coefficient α) allowing acquisition of information about the viscous component, was used (17). The three rheological parameters (shear stiffness, viscosity, and alpha parameter for springpot) were identified for each model.

Finally, the viscoelastic (μ , η) properties of the liver were analyzed as a function of the method and as a function of the rheological model.

Statistical Analysis

Unpaired t -tests were made to analyze the elastic and viscous behaviors, from experimental MRE cartographies and from rheological models as a function of the level of fibrosis. Subsequently, paired t -tests were performed in order to compare the viscosities calculated from both methods for each level of fibrosis. The statistical analysis was significant for $P < 0.05$ using the software Statgraphics 5.0 (Sigma Plus, Maryland, USA).

RESULTS

The postprocessing, comprised of the IA and rheological models, is a key step in liver diagnosis. Therefore,

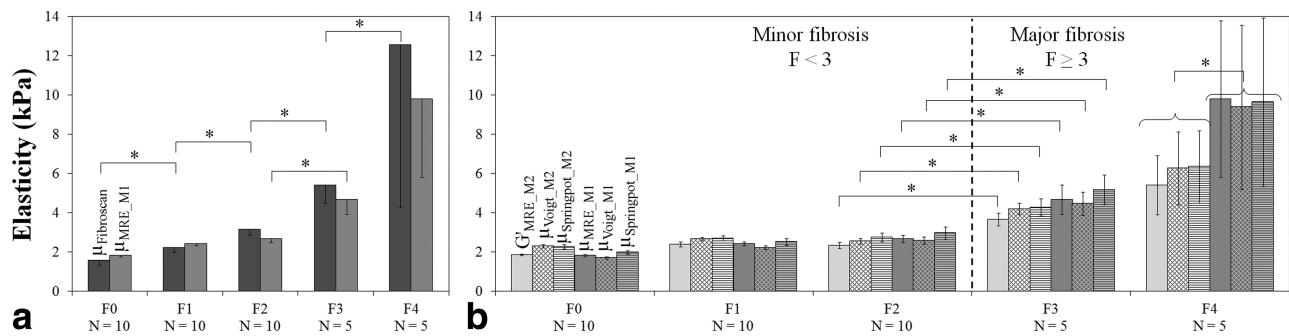


Figure 2. A: Experimental elasticity obtained with both elastography techniques, the Fibroscan (50 Hz) and the MRE techniques (60 Hz), as a function of the level of fibrosis. **B:** Comparison of experimental ($\mu_{\text{MRE_M1}}$ and $G'_{\text{MRE_M2}}$) and rheological ($\mu_{\text{models_M1}}$ and $\mu_{\text{models_M2}}$) elasticities from two different (M1 and M2) MMRE postprocessings at a clinical frequency of 60 Hz.

the following results will increase radiologist's awareness of the implemented postprocessing in the MRI machine.

Characterization of the Elastic Liver Properties

It must be noted that the effect of postprocessing on the elasticity results was analyzed for the frequency 60 Hz due to the clinical liver MRE test performed at this optimal frequency (17).

Comparison of the Liver Elasticity Between the Elastography Techniques

The experimental elasticities obtained with the Fibroscan ($\mu_{\text{Fibroscan}}$) technique at 50 Hz and the MRE ($\mu_{\text{MRE_M1}}$) at 60 Hz were in the same range for each fibrosis level (Fig. 2A) as found in the literature (3,5). A significant ($P < 0.05$) increase was found between the different stages of fibrosis for the Fibroscan and between minor and major fibrosis for the MRE technique. A similar significant ($P < 0.05$) increase was also observed for the rheological elasticities (Fig. 2B) between minor and major fibrosis. A higher increase of the shear stiffness, for alcoholic patients stage F4, was not significant due to the composition of this group made up of more severe fibrosis and the low number of F4 patients. In addition, the comparison of the standard deviation for severe fibrosis F4 revealed a higher variation for the Fibroscan (Fig. 2A).

Effect of the Rheological Models

The prescribed rheological models were useful for the second method (M2) enabling measurement of the elasticity ($\mu_{\text{models_M2}}$: $\mu_{\text{Voigt_M2}}$ and $\mu_{\text{Springpot_M2}}$) (Fig. 1G) instead of an elasticity tendency represented by the cartography $G'_{\text{MRE_M2}}$ (Fig. 1B).

Method 2 showed similar range of values for the elasticity calculated with the two rheological models ($\mu_{\text{Voigt_M2}} = \mu_{\text{Springpot_M2}}$) (Figs. 2B, 3A). In addition, the comparison of elasticity obtained experimentally at 60 Hz ($G'_{\text{MRE_M2}}$) and with rheological models ($\mu_{\text{models_M2}}$) revealed similar values ($G'_{\text{MRE_M2}} = \mu_{\text{models_M2}}$) attesting that the trend of elasticity closely revealed the liver elasticity behavior (Figs. 2B, 3B). It can be concluded that the present rheological models

had no influence on the range of elasticity using the second method.

Subsequently, the local experimental elasticity ($\mu_{\text{MRE_M1}}$ at 60 Hz, Fig. 1A) obtained from Method 1 along the prescribed profile was also calculated with the same rheological models ($\mu_{\text{Voigt_M1}}$, $\mu_{\text{Springpot_M1}}$) and similar elasticities were obtained ($\mu_{\text{Voigt_M1}} = \mu_{\text{Springpot_M1}}$) (Figs. 2B, 3C). Moreover, the comparison of elasticity between the experimental ($\mu_{\text{MRE_M1}}$) and rheological ($\mu_{\text{models_M1}}$) analyses revealed equivalent range of values ($\mu_{\text{MRE_M1}} = \mu_{\text{models_M1}}$) (Figs. 2B, 3D). It can be concluded that the present rheological models had no influence on the local elasticity measurement.

This analysis demonstrated that the use of rheological models had no effect on the elasticity results regardless of the analysis methods used, eg, with or without an inversion algorithm.

Effect of the Methods (M1: with IA and M2: without IA)

The comparison of elasticity (60 Hz) between the experimental methods ($\mu_{\text{MRE_M1}}$ vs. $G'_{\text{MRE_M2}}$, Fig. 3E) and rheological methods ($\mu_{\text{models_M1}}$ vs. $\mu_{\text{models_M2}}$, Fig. 3F) revealed similar ranges of data for fibrosis ($F \leq 3$). Thus, the local elasticity values ($\mu_{\text{MRE_M1}}$, Fig. 2B) were similar to the trend of elasticity represented by the cartography $G'_{\text{MRE_M2}}$ until fibrosis $F \leq 3$ (Fig. 2B). For severe fibrosis (F4), Method 1 revealed a significant ($P < 0.05$) higher experimental ($\mu_{\text{MRE_M1}}$) and rheological ($\mu_{\text{models_M1}}$) elasticities compared to those obtained with Method 2 ($G'_{\text{MRE_M2}}$ and $\mu_{\text{models_M2}}$) (Fig. 2B).

It can be concluded that Method 1, which did not apply an inversion algorithm, increased the result of the elasticity values for the severe stage of fibrosis (F4).

Characterization of the Viscous Liver Properties

Analysis of the Experimental Trend of Viscosity (G'')

The experimental viscosity cannot be calculated at a unique frequency 60 Hz without the use of an inversion algorithm (Fig. 1A, Method 1). However, the experimental viscous tendency ($G''_{\text{MRE_M2}}$) of the liver was obtained with the second method (M2) using an inversion algorithm. The results showed a slight increase in the $G''_{\text{MRE_M2}}$ trend until the level of fibrosis F3 and a higher increase for severe F4 fibrosis (Fig. 4A).

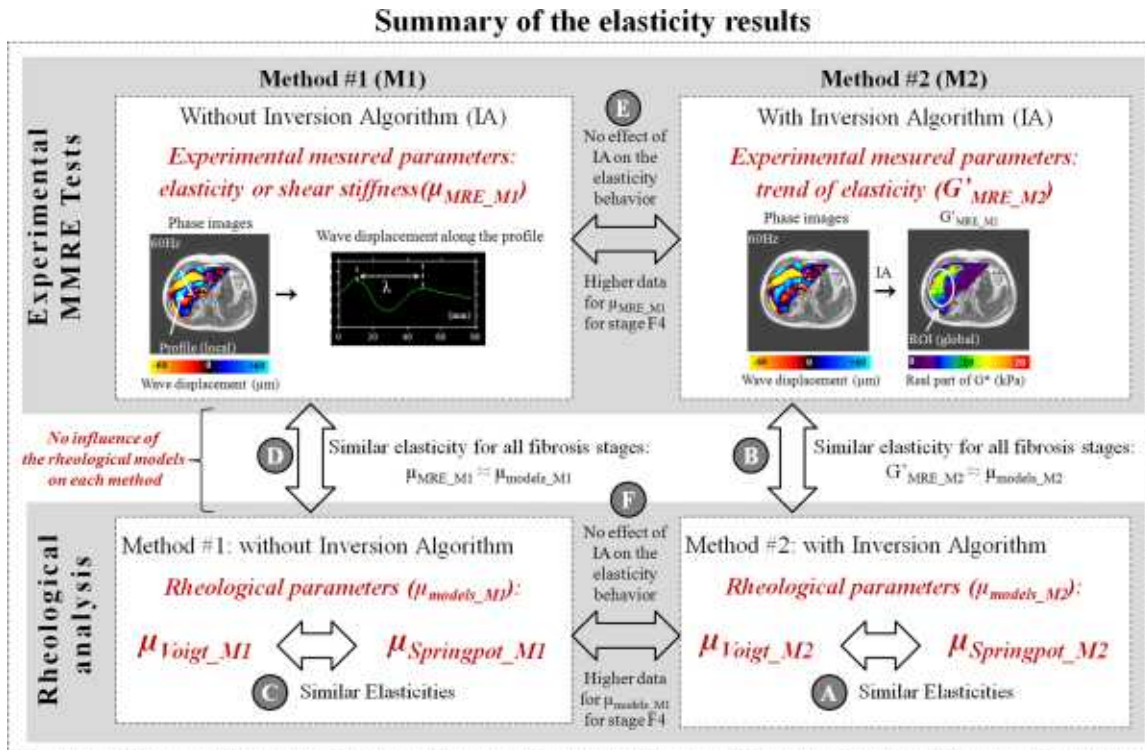


Figure 3. Summary of the effect of the MMRE postprocessing on the elastic properties of the liver. The main conclusions are written in the diagram and identified with different letters. [Color figure can be viewed in the online issue, which is available at wileyonlinelibrary.com.]

Effect of the Rheological Models

As no experimental viscous data was recorded with Method 1, the use of rheological models allowed for the measurement of the viscosity (η_{models_M1} : η_{Voigt_M1} and $\eta_{Springpot_M1}$, Fig. 1F) which slightly increased until the level of fibrosis F3 and which was highly increased for severe fibrosis (F4) (Fig. 4B).

For each method (M1 and M2), the viscosity data measured with the springpot model revealed significantly ($P < 0.05$) higher viscosity values ($\eta_{Springpot_M1, M2} > \eta_{Voigt_M1, M2}$) compared to those calculated with Voigt model (Figs. 4B, 5A).

The comparison between viscosities (G''_{MRE_M2} and η_{models_M2}) obtained with Method 2 (Fig. 5B) revealed different viscous behaviors. Indeed, the experimental

viscous tendency (G''_{MRE_M2}) increased as a function of the fibrosis level while the numerical viscosity (η_{models_M2}) remained constant with the stage of fibrosis (Fig. 4B). It can be concluded that the rheological models had an effect on the viscosity behavior from Method 2.

Effect of the Methods (M1: without IA and M2: with IA)

The use of Method 1 revealed a slight increase of the viscosity (η_{models_M1}) until the fibrosis level (F < 3), followed by a higher increase of viscosity for the major fibrosis (F3, F4) (Fig. 4B).

Conversely, the use of Method 2 revealed a range of viscosity (η_{models_M2}) that did not vary with the severity of the fibrosis (Fig. 4B).

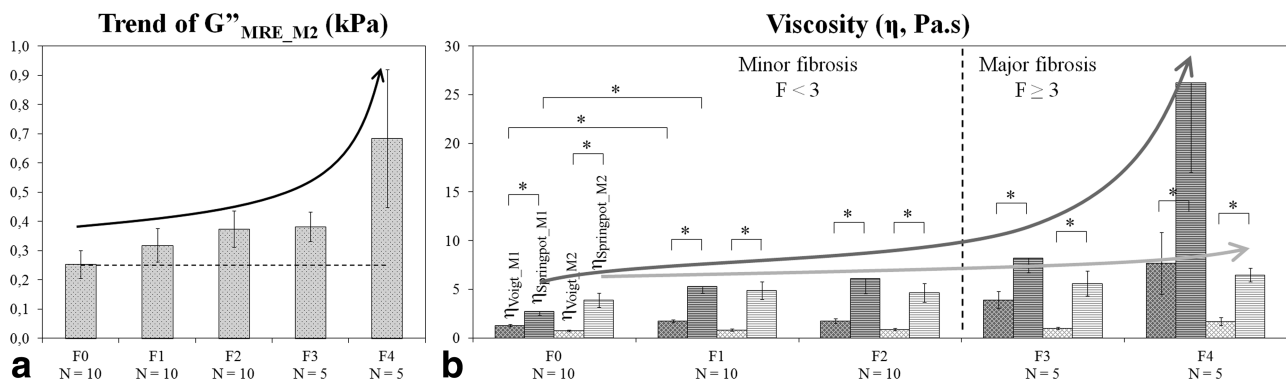


Figure 4. A: Behavior of the experimental viscous tendency as a function of the level of fibrosis. **B:** Comparison of the viscosity (η_{models_M1} and η_{models_M2}) from two different (M1 and M2) MMRE postprocessings at a clinical frequency of 60 Hz.

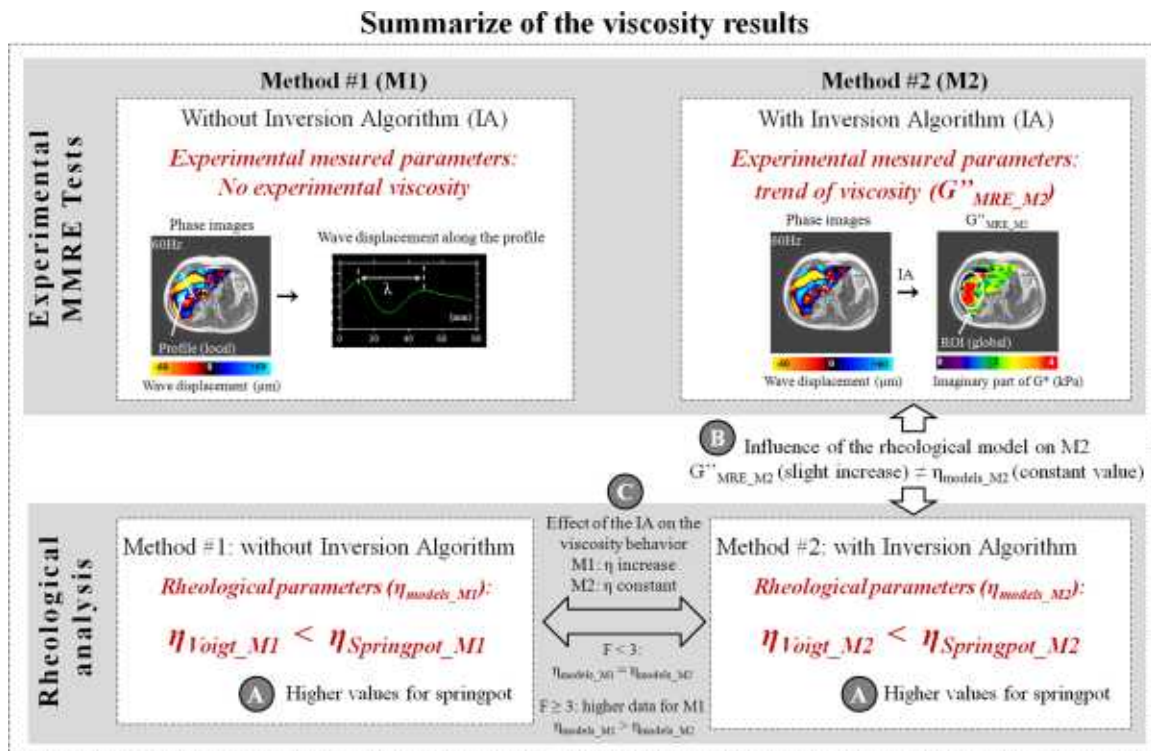


Figure 5. Summary of the effect of MMRE postprocessing on the viscous properties of the liver. The main conclusions are added in the diagram and identified with different letters. [Color figure can be viewed in the online issue, which is available at wileyonlinelibrary.com.]

The comparison of the methods (Fig. 5C) demonstrated the same range of viscosity ($\eta_{models_M1} = \eta_{models_M2}$) (Fig. 4B) for minor fibrosis ($F < 3$) while major fibrosis (F3, F4) exhibited higher viscosity values with the use of Method 1 ($F \geq 3$: $\eta_{models_M1} > \eta_{models_M2}$).

It can be concluded that there is an effect of the method used on the viscosity. Indeed, Method 1, which did not use an inversion algorithm, showed an increase of viscosity as a function of the level of fibrosis, while Method 2 (composed of an inversion algorithm) provided a constant viscosity regardless of the severity of liver fibrosis.

DISCUSSION

The MRE technique arose in the radiology community as a clinical tool to help clinicians to noninvasively diagnose liver fibrosis. In order to increase radiologist's awareness of the effect of the MRE postprocessing (inversion algorithm, rheological model) on the diagnostic result, a brief review of the MRE data analysis is provided.

At the beginning of the MRE, quantification of the fibrosis was performed with a local measurement of the elasticity within the liver at a unique frequency (60 Hz) (2). This elasticity was directly calculated from the phase images with a profile placed locally in the direction of the wave propagation (as the present Method 1). However, this type of analysis would have been a waste of time for the radiologist who should have been trained to analyze the phase image. Therefore,

inversion algorithms were developed to make characterization of the liver elasticity easier (11) and a cartography (G') revealing the elastic tendency of the liver tissue was developed (as the present Method 2). Thus, a radiologist could spatially measure the elastic properties within different ROIs.

However, this MRE postprocessing raised the following question: Is the cartography of elasticity (G') damaged by the use of an inversion algorithm? To answer to this question, the present study demonstrated that the use of an inversion algorithm did not change the liver elastic behavior, which increased as a function of the level of fibrosis. However, it must be noted that the elastic values from the cartography (G') were underestimated for severe fibrosis F4, possibly due to the prescribed ROI, which integrated an average value of different elasticities. Therefore, to accurately diagnose a suspicious area, in a case of severe fibrosis, the radiologists may use the local analysis corresponding to the initial postprocessing similar to the present Method 1. This result showed the complementarity of MRE postprocessing for the purpose of characterizing the elastic properties of the liver.

In addition to the elastic properties, the characterization of the viscous properties allowed quantification of the viscoelastic (elasticity and viscosity) behavior of the liver, which can be used for the development of accurate surgical simulation tools (19,20). In the literature, viscosity was also measured in a few MMRE studies using different frequencies (25, 37.5, 50, and 62.5 Hz) than the present study (60, 70, and 80 Hz), and another type of driver (12,15,16,21). Moreover,

these previous works also applied several rheological models (Zener, Voigt, springpot) in order to quantify the viscosity for liver disease using postprocessing similar to the present Method 2.

However, conflicting results were published about the viscosity behavior as a function of the fibrosis level. Indeed, using the springpot model, Klatt et al's study (21) fixed a same viscosity value (1 Pa.s) for the healthy and pathological livers similar to Asbach et al's study (12) which fixed this parameter at a higher value (7.3 Pa.s). It can be stated that the viscosity behavior remained constant as a function of the level of fibrosis. The present study was in agreement with this statement because the viscosity calculated with Method 2 and the springpot model ($\eta_{\text{springpot_M2}}$) remained constant with the degree of fibrosis. The present average viscosity was 5.2 ± 2.5 Pa.s and this value was closer to Asbach et al's study (7.3 Pa.s). The Voigt model was also used in Klatt et al's study (15), who found a lower value (2.8 ± 0.3 Pa.s) of the healthy viscosity compared to Asbach et al's study (7.3 Pa.s) which used the springpot model. The present study also revealed lower healthy viscosity values using the Voigt model ($\eta_{\text{Voigt_M2}} = 0.8 \pm 0.1$ Pa.s) compared to the springpot model ($\eta_{\text{springpot_M2}} = 3.9 \pm 0.7$ Pa.s).

It was expected that the microstructural changes occurring in severe fibrosis would be revealed by a variation of the viscosity value. In contrast with previous studies, in 2008 Asbach et al, using the Zener model, found an increase of the viscosity value between the healthy (7.3 Pa.s) and the pathological (14.4 Pa.s) livers (16). The same behavior was found with the present study, which showed an increase of the viscosity ($\eta_{\text{models_M1}}$), using the Method 1, for severe fibrosis.

In conclusion, this study demonstrated the impact of MMRE postprocessing on the viscosity behavior and reveals new insights for radiologists who should be vigilant before using viscosity as an additional diagnostic marker. Moreover, it will also be necessary to perform a cross-correlation of the present viscosity parameter with another in vivo imaging technique. The viscosity requires further analyses to prove its relevance in clinical practice compared to the elastic measurement, which was not influenced by the different MMRE postprocessing methods until stage F3 and therefore remains the clinical reference parameter to noninvasively diagnose liver fibrosis for a clinical MRE test.

ACKNOWLEDGMENT

We thank Dr. R.L. Ehman at the Mayo Clinic, Department of Radiology, for MR support technology.

REFERENCES

1. Friedman SL. Mechanisms of hepatic fibrogenesis. *Gastroenterology* 2008; 134:1655–1669.

2. Rouvière O, Yin M, Dresner MA, et al. MR elastography of the liver: preliminary results. *Radiology* 2006; 240:440–448.
3. Bensamoun SF, Wang L, Robert L, Charleux F, Latrive J-P, Ho Ba Tho M-C. Measurement of liver stiffness with two imaging techniques: magnetic resonance elastography and ultrasound elastometry. *J Magn Reson Imaging* 2008; 28:1287–1292.
4. Roulot D, Czernichow S, Le Clésiau H, Costes JL, Vergnaud AC, Beaugrand M. Liver stiffness values in apparently healthy subjects: influence of gender and metabolic syndrome. *J Hepatol* 2008; 48:606–613.
5. Huwart L, Sempoux C, Vicaux E, et al. Magnetic resonance elastography for the noninvasive staging of liver fibrosis. *Gastroenterology* 2008; 135:32–40.
6. Rustogi R, Horowitz J, Harmath C, et al. Accuracy of MR elastography and anatomic MR imaging features in the diagnosis of severe hepatic fibrosis and cirrhosis. *J Magn Reson Imaging* 2012; 35:1356–64.
7. Bensamoun SF, Leclerc GE, Debernard L, Cheng X, Robert L, Charleux F, Rhein C, Latrive JP. Cut-off values for alcoholic liver fibrosis using magnetic resonance elastography technique. *Alcoholism: Clin Exp Res* 2012. In press.
8. Venkatesh SK, Yin M, Glockner JF, et al. MR elastography of liver tumors: preliminary results. *Am J Roentgenol* 2008; 190:1534–1540.
9. Motosugi U, Ichikawa T, Amemiya F, et al. Cross-validation of MR elastography and ultrasound transient elastography in liver stiffness measurement: discrepancy in the results of cirrhotic liver. *J Magn Reson Imaging* 2012; 35:607–610.
10. Nguyen-Khac E, Chatelain D, Tramier B, et al. Assessment of asymptomatic liver fibrosis in alcoholic patients using fibroscan: prospective comparison with seven non invasive laboratory tests. *Aliment Pharmacol Ther* 2008; 28:1188–1198.
11. Manduca A, Oliphant TE, Dresner MA, et al. Magnetic resonance elastography: non-invasive mapping of tissue elasticity. *Med Image Anal* 2001; 5:237–254.
12. Asbach P, Klatt D, Schlosser B, et al. Viscoelasticity-based staging of hepatic fibrosis with multifrequency MR elastography. *Radiology* 2010; 257:80–86.
13. Salameh N, Peeters F, Sinkus R, et al. Hepatic viscoelastic parameters measured with MR elastography: correlations with quantitative analysis of liver fibrosis in the rat. *J Magn Reson Imaging* 2007; 26:956–962.
14. Van Beers B, Doblaz S, Sinkus R. New acquisition techniques: fields of application. *Abdom Imaging* 2012; 37:155–163.
15. Klatt D, Hamhaber U, Asbach P, Braun J, Sack I. Noninvasive assessment of the rheological behavior of human organs using multifrequency MR elastography: a study of brain and liver viscoelasticity. *Phys Med Biol* 2007; 52:7281–7294.
16. Asbach P, Klatt D, Hamhaber U, et al. Assessment of liver viscoelasticity using multifrequency MR elastography. *Magn Reson Med* 2008; 60:373–379.
17. Leclerc GE, Debernard L, Foucart F, et al. Characterization of a hyper-viscoelastic phantom mimicking biological soft tissue using an abdominal pneumatic driver with magnetic resonance elastography (MRE). *J Biomech* 2012; 45:952–957.
18. Bourbié T, Coussy O, Zinszner B. *Acoustique des milieux poreux*. Publications de l'IFP, Collection Science et Technique du pétrole, Editions Technip. Paris; 1986.
19. Schwartz J-M, Denninger M, Rancourt D, Moisan C, Laurendeau D. Modelling liver tissue properties using a non-linear visco-elastic model for surgery simulation. *Med Image Anal* 2005; 9:103–112.
20. Haghpanahi M, Naeeni HA. Investigation of viscoelastic properties of human liver tissue using MR elastography and FE modeling. 17th Iranian Conference of Biomedical Engineering (ICBME), 2010, p. 1–4.
21. Klatt D, Asbach P, Somasundaram R, Hamm B, Braun J, Sack I. Untersuchung des Fest-flüssig-Materialverhaltens der Leber zur nicht invasiven Diagnose diffuser Lebererkrankungen mittels Magnetresonanz-Elastografie. *RöFo* 2008; 180:1104–1109.